FULL ELECTROMAGNETIC FEL SIMULATION VIA THE LORENTZ-BOOSTED FRAME TRANSFORMATION *

W.M. Fawley, J.-L. Vay, LBNL, Berkeley, CA 94720, USA†

Abstract

Numerical electromagnetic simulation of some systems containing charged particles with highly relativistic directed motion can by speeded up by orders of magnitude by choice of the proper Lorentz-boosted frame [1]. A particularly good application for calculation in a boosted frame is that of short wavelength free-electron lasers (FELs) where a high energy electron beam with small fractional energy spread interacts with a static magnetic undulator. In the optimal boost frame (*i.e.*, the ponderomotive rest frame), the red-shifted FEL radiation and blue-shifted undulator field have identical wavelengths and the number of required longitudinal grid cells and time-steps for fully electromagnetic simulation (relative to the laboratory frame) decrease by factors of γ^2 each. In theory, boosted frame EM codes permit direct study of FEL problems for which the eikonal approximation for propagation of the radiation field and wiggler-period-averaging for the particle-field interaction may be suspect.

We have adapted the WARP code [2] to apply this method to several electromagnetic FEL problems including spontaneous emission, strong exponential gain in a seeded, single pass amplifier configuration, and emission from e-beams in undulators with multiple harmonic components. WARP has a standard relativistic macroparticle mover and a fully 3-D electromagnetic field solver. We discuss our boosted frame results and compare with those obtained using the "standard" eikonal FEL simulation approach.

INTRODUCTION

It is well known that in general, explicit, fully electromagnetic simulation will have its time step Δt limited by the Courant condition corresponding to the numerical grid spacing and/or that necessary to achieve sufficient temporal resolution of the highest frequencies important to the physics of the particular situation. For problems in which a highly relativistic charged particle beam is present, the overall system time and/or length scale L_{sim} can be large and the ratio of scale lengths $L_{sim}/c\Delta t$ can become enormous. Recently, Vay [1] pointed out that for some of these problems performing the simulation in a Lorentz-boosted frame offers potentially orders of magnitude speed-up in computation time.

Optical and shorter wavelength FEL's whose ratio of wiggler length L_w to radiation wavelength λ_R can easily exceed 10^7 or greater are obvious candidates for boosted frame calculation. The natural boosted frame for FEL computations is the so-called "ponderomotive" frame in which the e-beam's longitudinal speed in the undulator is zero on average. In this frame the red-shifted FEL resonant wavelength $\lambda'_R = 2\gamma_F\lambda_R$ is equal to the blue-shifted undulator wavelength $\lambda'_u = \lambda_u/\gamma_F$. Here $\gamma_F^2 \equiv \gamma_0^2/(1+a_u^2)$ with a_u being the normalized, RMS undulator strength. The undulator shrinkage and radiation wavelength increase result in an overall decrease of the needed number of longitudinal grid zones by a factor $\approx 2\gamma_F^2$. Likewise, from the point of view of the Courant condition, the increase in λ'_R permits (in general) a similar increase in the time step and together with the reduced undulator length gives another factor of $2\gamma_F^2$ savings, so that the overall savings in CPU time relative to a lab frame EM code can scale with γ_F^4. However, in cases where the electron beam length l_b sets required simulation z-size (via use of a moving window), the reduction factor may only be $\sim \gamma_F^2$. If one requires the transverse grid spacing to be $\sim 10\Delta z$ or less, one gains even larger savings in memory and CPU requirements.

Relative to wiggler-period averaged eikonal codes such as GINGER, GENESIS, FAST, *etc.*, that permit effective longitudinal grid sizes $\Delta z \sim 0.1 L_{gain} \approx 10\lambda_w/\rho$, the lab-equivalent grid zone size in boosted frame codes is 1-3 orders of magnitude smaller, depending upon what harmonic must be resolved. Similarly, a boosted frame code requires full frequency bandpass $\sim 10c/\lambda_R$ whereas eikonal codes can have much smaller ones with $\Delta\nu \sim 10\rho\lambda_R/c$. Here ρ is the standard FEL parameter. Due to the parabolic nature of the EM equations in eikonal codes, there is in general also no numerical problem in taking a large ratio for transverse-to-longitudinal grid sizes (but one must of course resolve the transverse e-beam size). Consequently, boosted frame EM codes will still be very much slower (and have much, much larger memory requirements) than standard FEL codes, despite their impressive speed-up over lab frame full EM codes. On the other hand, for certain problems such as spontaneous emission, ultrashort electron beam pulses, and high diffraction cases where the paraxial approximation begins to fail, the limited frequency bandpass and angular resolution of eikonal codes limit their accuracy and a boosted frame approach permits study of such problems not feasible with a standard EM code operating in the lab frame. A third approach [3] effectively retains the full field equation but drops non-paraxial source terms also permits study of problems such as spontaneous emission.

* This work was supported under the auspices of the Office of Science, U.S. DOE under Contract No. DE-AC02-05CH11231 and also used resources the National Energy Research Scientific Computing Center.

† WMFawley@lbl.gov

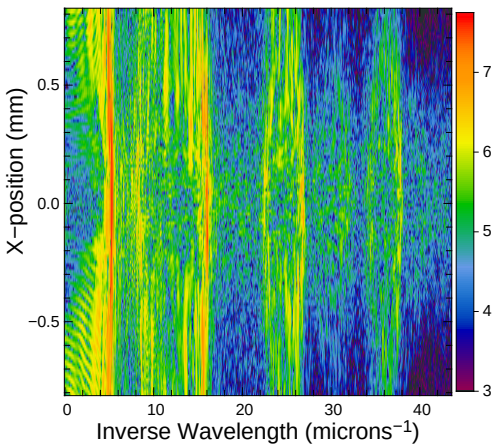

Figure 1: False color-coded (log10 intervals) spontaneous emission spectrum $I(\lambda^{-1})$ determined on the $x-z$ plane with $y = 0$ from a full 3D, boosted frame WARP simulation of 100 mA e^-, e^+ beams propagating together in a 20-period undulator resonant at $\lambda_R = 200\,\mathrm{nm}$.

To study various FEL problems in the boosted frame, we used the WARP simulation code [2] with its standard full 3-D EM solver together with special Python-language scripts to implement linearly-polarized undulator and seed laser fields in the boosted frame. In addition to WARP's normal extensive particle and field diagnostic suite, we measured the forward radiation intensity and on-axis far field radiation through transverse planes fixed in the lab frame (*e.g.*, at a fixed z relative to the undulator entrance). For most problems we chose $\Delta z' = c\Delta t' = \lambda'_R/M$ with M in the range 16 to 32 to ensure reasonable evaluation of third harmonic emission. For simplicity and increased computational speed, in many cases we adopted 2-D slab-mode geometry (*e.g.*, $x-z$ or $y-z$). For both 2- and 3-D simulations we used transverse grid sizes $\sim O(1-8)\times\Delta z'$. In order to avoid explicit initialization of the E- and B-fields associated with a beam pulse with a net current and charge, at $t' = 0$ we added a "ghost" positron beam with the exact same charge and current distribution as the nominal electron beam (see [4] for some additional details and also some previous simulation results regarding prebunched beams). This choice neglects the longitudinal space charge fields that can occur for very high current situations (*e.g.*, the Raman regime). We now present some boosted frame results for spontaneous emission, a high gain seeded amplifier, and emission by pre-bunched beams in "biharmonic" undulators.

SPONTANEOUS EMISSION

Spontaneous emission from a very low current beam provides a good test case for EM and FEL simulation codes as one expects the overall emission to grow linearly with beam charge and undulator length. We used WARP to simulate a 8-μm-long, 100-mA particle current (for both the e^- and e^+ components), 180.2-MeV energy, 1.0 mm-mrad emittance beam propagating through an 25-mm period, 0.5-m long, linearly-polarized undulator (y-wiggle plane) with $a_u = 1$ and $\lambda_R = 200\,\mathrm{nm}$. Transforming to the boost frame with $\gamma_F = 250$ gives $\lambda'_R = \lambda'_u = \lambda_u/\gamma_F = 100\,\mu\mathrm{m}$ and $L'_u = 2\,\mathrm{mm}$. With $\sigma_x = \sigma_y = 120\,\mu\mathrm{m}$, we chose a 3D grid extending transversely to $\pm 0.8\,\mathrm{mm}$ and $\Delta x, y = 12.5\,\mu\mathrm{m}$. With such a small current and beam-length, we used the actual number of electrons (≈ 20800) loaded randomly with a 4D transverse and waterbag longitudinal distributions.

Figure 1 shows the $x-$ and $\lambda-$resolved output near-field output spectrum, determined (approximately) by taking a Fourier transform in z in the boosted frame of $E_y - c\beta_F \times B_x$ along $y = 0$. One sees relatively strong fundamental emission at $\lambda = 200\,\mathrm{nm}$ and also obvious third and fifth harmonic emission, more confined toward the axis. Due both to the relatively small a_u and the choice of $\Delta z' = \lambda'_R/32$, emission at seventh and higher harmonics will be numerically suppressed. Diagnostics of the total positive-z directed flux at various locations in the undulator quantitatively are smaller for these particular parameters by a factor of ~ 2.5 than the analytical expectation. We believe there are at least two reasons for this discrepancy: 1) The non-zero transverse beam and grid zone size leads to some numerical suppression of off-axis emission by destructive interference effects; we have seen this effect previously in slab-mode simulations of coherent emission from low current, ultrashort pulses with $\sigma_z \ll \lambda_R$. Decreasing $\sigma_{x,y}$ to $40\,\mu\mathrm{m}$ drops the power discrepancy to a factor of 1.5 or so but worsens the next problem: 2) The much smaller Fresnel number in the boosted frame leads to significant radiation propagating at a much larger angle relative to the $z-$ axis than is true in the lab frame leading to some power escaping transversely; there is also "$\cos\theta$" diagnostic undercounting issue. For larger Fresnel numbers, the spontaneous power does scale linearly with undulator length as expected. Altogether then, we believe these boosted frame spontaneous emission results are reasonably accurate but one must take care in terms of diagnosing emission propagating in the boosted frame at large angles off-axis.

HIGH GAIN FEL AMPLIFIER SIMULATION IN THE BOOSTED FRAME

At the other extreme from the low current spontaneous emission case is that of a single pass, high gain FEL amplifier with gain length $L_g \ll L_u$. We have done a number of simulations studying a MOPA configuration at $\lambda_R = 200\,\mathrm{nm}$ using similar undulator and beam parameters except the current has been increased to the kA range and we have add 10-MW seed laser with a Gaussian waist size of $250\,\mu\mathrm{m}$. Figure 2 shows results from a 2-D (slab mode) boosted frame simulation with $I_B = 1\,\mathrm{kA}$ (each for the separate e^- and e^+ components), an effective $y-$ size of $120\,\mu\mathrm{m}$, and $\Delta x = \Delta z' = \lambda'_R/24$. The left plot

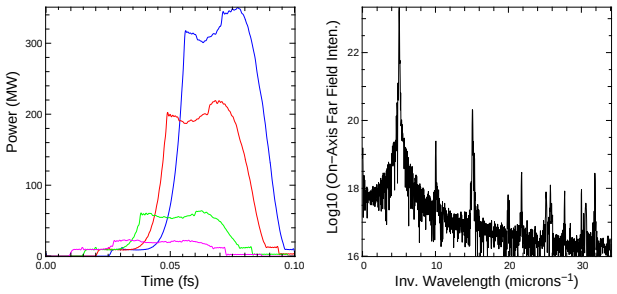

Figure 2: Boosted frame simulation results for a FEL amplifier seeded with 10 MW of input power at 200-nm wavelength. The left plot shows increasing $P(t)$ traces at $z = [0.5, 0.7, 0.9, 1.0]$ m. The right plot shows the on-axis, far field spectrum (a.u.) for $z = 1.0$ m.

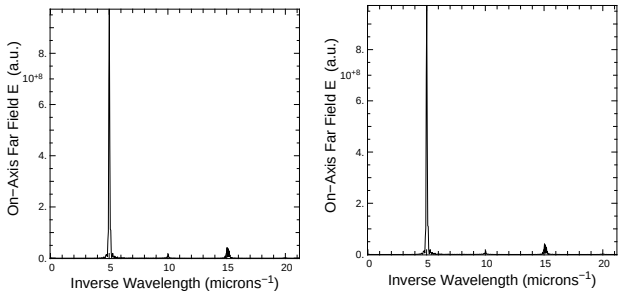

Figure 3: On-axis, far field spectrum $|E(\omega)|$ from a pre-bunched beam propagating in (left plot) a "normal", single frequency undulator with $a_{u,1} = 1.0$ and (right plot) a in biharmonic undulator with $\lambda_{u,2} = 3\lambda_{u,1}$, $a_{u,1} = 1.0$ and $a_{u,2} = 1.5$.

shows $P(z,t)$ at four locations in the lab frame within the 1-m long undulator; the peak power at undulator exit is $\approx$ 350 MW and the effective L_g is $\approx$ 0.165 m. The right plot shows the spectrum of the on-axis far field radiation. Relative to the power level of the fundamental, the third harmonic is at a level of $\approx$ 0.1% while the second and fourth harmonics are down by one and two additional orders of magnitude, respectively. A time-steady benchmark run with the GINGER code in slab-mode geometry with $I_B = 2$ kA shows slightly greater gain for the same beam parameters with $L_g = 0.156$ m. However, there is a $\approx 10\%$ uncertainty regarding L_g due to possible differences between the effective transverse distributions at given z's in the lab frame so it is premature to speculate on differences due to transverse space charge effects or issues arising from the extremely high gain. The GINGER run shows third harmonic power at a level 0.4% that of the fundamental or nearly a factor of 4 higher than that in the boosted frame run. Some of this difference can be attribued to the relatively large time step vis-avis $\lambda_R'/3c$.

We have also done a full 3-D run with similar parameters except the current for both the boosted frame and GINGER simulations were increased by a factor of two to counteract increased diffractive losses. At the end of the undulator, WARP shows 80 MW of power while GINGER gives 191 MW; equivalently, the power gain lengths are 0.22 and 0.18 m, respectively. For another independent check, the empirical Xie gain fitting formula [5] predicts a power gain length of 0.17 m. As we indicated above, it as yet remains premature to associate this 20% difference in L_g to physically real effects such as space charge or extremely high gain corrections.

EMISSION BY A PREBUNCHED BEAM IN A BIHARMONIC UNDULATOR

Several authors have discussed the possible utility of a biharmonic undulator configuration (see., *e.g.*, Refs. [6]-[9]) where the magnetic vector potential strength $\vec{A} = \vec{A}_1 \cos(k_{u,1}z + \phi_1) + \vec{A}_2 \cos(k_{u,2}z + \phi_2)$ and $k_{u,1}$ and $k_{u,2}$ are related harmonically, *e.g.*, to enhance third harmonic emission. Another possible use of a biharmonic configuration is to provide an additional "source" of A for an externally seeded FEL amplifier where the electron beam energy must remain fixed (*e.g.*, the accelerator is feeding a multiplexed set of FEL's operating simultaneously). Then the maximum output radiation wavelength of a particular undulator depends upon the peak value of normalized undulator strength a_u available at minimum gap closure g_{min}. If the "primary" undulator has a short $\lambda_{u,1}$ and a peak on-axis value of $a_{u,1}$ limited physically to not much more than 1 because $k_{u,1}g_{min} \geq 2$, there will be a small effective tuning range in λ_R. Adding a "secondary", variable strength undulator field A_2 with a longer period can strongly increase the maximum reachable wavelength if $\max|A_2| \geq 2\max|A_1|$ because the FEL resonance relation (at the shorter resonant wavelength) obeys

$$\lambda_{R,1} = \frac{\lambda_{u,1}}{2\gamma^2} \times \left(1 + a_{u,1}^2 + a_{u,2}^2\right) \qquad (1)$$

Note that from a mathematical point of view, there is no requirement that the two undulators be related harmonically, although from a construction point of view this choice may be easiest to implement. Also, the polarity of the two undulators can be entirely different (*e.g.*, cross-polarized linear undulators).

Modeling FEL radiation emission in such a configuration poses accuracy issues for eikonal codes employing the standard wiggle-period-averaging approximation unless $\lambda_{u,2} \gg \lambda_{u,1}$. For linear undulators, the "JJ" Bessel function difference term also needs to be modified because of dephasing associated with the wiggle motion due to $\vec{A}_2$. There also can be harmonic coupling if $\lambda_{u,2}$ is an integer harmonic of $\lambda_{u,1}$. This difficulty does not arise for boosted frame EM simulation so long as the effective temporal and spatial gridding supports the shortest radiation wavelengths of interest.

We did a series of slab-mode, boosted frame simulations for a 1-A, 40-fs (waterbag profile), 180-MeV e-beam propagating in a $0.75-$m length biharmonic undulator with

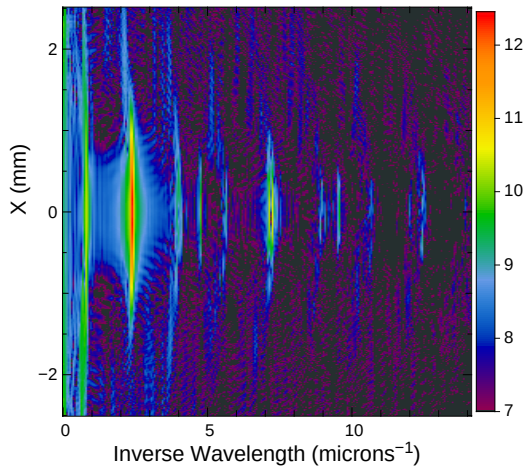

Figure 4: False color-coded (log10 intervals), near field emission spectrum from the boosted frame 2D simulation of the biharmonic undulator corresponding to the right plot of Fig. 3.

$\lambda_{u,1} = 25\,\mathrm{mm}$, $a_{u,1}$=1.0, $\lambda_{u,2} = 75\,\mathrm{mm}$, and $a_{u,2}$ ranging from 0 to 1.5. We prebunched the beam over $\pi/4$ in phase at $\lambda_{R,1}$ which, using Eq. 1, increased from 200 to 425 nm, and set $c\Delta t' = \lambda'_{R,1}/24$. In Fig. 3 we plot the on-axis electric field spectrum just outside the undulator with $a_{u,1} = 1.0$ in both of the following two cases: $a_{u,2} = 0$ (left plot) and $a_{u,2} = 1.5$ (right plot). As expected, the biharmonic case shows the fundamental photon energy shifting redwards by a factor of $4.25/2$ but the relative spectral width appears unchanged. The biharmonic case also shows a greater relative strength of the third harmonic and there is a somewhat greater amount of second harmonic (and sidebands to either side). However, the far field power in the dominant mode is down by more than an order of magnitude when compared to the simple, monoharmonic undulator case. The x-resolved near-field spectrum is plotted in Fig. 4 in logarithmic intervals to bring out more detail. The higher harmonics tend to be more confined to the central axis as one would expect from simple theory. If one looks closely, there is evidence of $x-$curvature for each of the spectral"lines" indicating red-shifting as one moves away from the x-axis. From these and related simple examples where we have varied the strength of $a_{u,2}$, we see that our expectations of tunability are confirmed although at a price of lowered power and richer emission spectrum. Since in general FEL gain increases significantly at longer wavelengths for a given set of electron beam parameters, the power loss as one tunes redward is not necessarily a showstopper. In the future we hope to do some additional studies of high gain, biharmonic MOPA configurations with external seeding to see how these and other effects play out.

DISCUSSION

Applying the Lorentz-boosted-frame simulation method to free-electron laser problems allows study of problems where the eikonal approximation method proves insufficient, *e.g.* those where the total emission bandpass is quite large, others where wiggler-period averaging is suspect, *etc*. As mentioned in the Introduction, use of the boosted frame transformation also allows direct EM simulation of very short wavelength FEL's with a huge ratio of L_u/λ_R. In our boosted-frame FEL studies to date we have been able to explore certain aspects of insertion device and FEL emission that are essentially "opaque" to standard FEL codes. Nonetheless, it is important to add that we have not uncovered any important critical physics that would make one doubt the basic correctness of the eikonal approximation or wiggler period-averaging for normal FEL problems. Although we have avoided problems for which space charge effects are very important, our simulation methods should treat them straight-forwardly presuming that the overall EM fields have been properly initialized. We have not as yet applied moving window or multigrid methods to help speed up FEL calculations even more in the boosted frame; in some different contexts (CSR emission [10] and LWFA simulations) such methods have proven useful. We have also modeled configurations in which the simulation window was chosen large enough in z' to contain all the electron beam and the equivalent slippage length in the boosted frame. For short undulators and short electron beams [*i.e.*, $N_u \leq 100,\ l_b \leq 2 \times l_{slip}$)], this is not too great a problem. However, for SASE configurations run to saturation or undulators with drift or chromatic dispersive sections, the longitudinal grid tends to become much larger. We are hopeful, though, that there exists one or more clever schemes to reduce the necessary simulation window by applying the equivalent of lab frame periodic boundary conditions.

ACKNOWLEDGEMENTS

We thank D. Grote for his continuing help in modification and use of the WARP code and also gratefully acknowledge use of parallel computational resources provided by LBNL's IT Division.

REFERENCES

[1] J.-L Vay, Phys. Rev. Lett. 98 (2007) 130405.

[2] D.P. Grote, A. Friedman, J.-L. Vay, and I. Haber, AIP Conf. Proc. 749 (2005), 55.

[3] L.T. Campbell, R. Martin and B.W.J. McNeil, Proc. FEL09 (Liverpool, UK; 2009), paper MOPC39.

[4] W.M. Fawley and J.-L. Vay, AIP Conf. Proc. 1086 (2009), 346.

[5] M. Xie, Nucl. Instr. Meth. A445 (2000), 59.

[6] D. Iracane and P. Bamas, Phys. Rev. Lett. 67 (1991), 3086.

[7] G. Dattoli and G. Voykov, Phys. Rev. E 48 (1993), 3030.

[8] M. Asakawa *et al.*, Nucl. Inst. Meth. A375 (1996) 416.

[9] G. Dattoli *et al.*, J. Appl. Phys. 100 (2006), 0804507.

[10] W.M. Fawley and J.-L. Vay, Proc. IPAC10 (Kyoto, Japan; 2010), paper TUPEC064.